Preparation and characteristics of Nb-doped indium tin oxide thin films by RF magnetron sputtering

LI Shi-na(李士娜)**, MA Rui-xin**(马瑞新)***, HE Liang-wei**(贺梁伟)**, XIAO Yu-qin**(肖玉琴)**, HOU Jun-gang**(侯军刚)**, and JIAO Shu-qiang**(焦树强)

Department of Non-ferrous Metallurgy, School of Metallurgical and Ecological Engineering, University of Science and Technology Beijing, Beijing 100083, China

Niobium-doped indium tin oxide (ITO:Nb) thin films are fabricated on glass substrates by radio frequency (RF) magnetron sputtering at different temperatures. Structural, electrical and optical properties of the films are investigated using X-ray diffraction (XRD), atomic force microscopy (AFM), ultraviolet-visible (UV-VIS) spectroscopy and electrical measurements. XRD patterns show that the preferential orientation of polycrystalline structure changes from (400) to (222) crystal plane, and the crystallite size increases with the increase of substrate temperature. AFM analyses reveal that the film is very smooth at low temperature. The root mean square (RMS) roughness and the average roughness are 2.16 nm and 1.64 nm, respectively. The obtained lowest resistivity of the films is $1.2 \times 10^{-4}\,\Omega \cdot cm$, and the resistivity decreases with the increase of substrate temperature. The highest Hall mobility and carrier concentration are 16.5 cm²/V·s and 1.88×10^{21} cm⁻³, respectively. Band gap energy of the films depends on substrate temperature, which is varied from 3.49 eV to 3.63 eV.

Transparent and conductive oxide (TCO) thin films have been the subject of intense research due to their importance in display and photovoltaic technologies[1-3]. More recently, TCOs have been used for flat panel displays, including liquid crystal displays, organic light emitting diodes and plasma displays. Among the various TCO thin films, tin doped indium oxide (ITO) is widely used in flat displays, solar cells, architectural glasses and other fields[4]. ITO film is a heavily doped and high-degenerate n-type semiconductor with a good electrical conductivity and transmittance in visible region, and it also has the resistance to chemical corrosion and good processing performance[5]. ITO films can be prepared by variety of techniques[6-12]. Magnetron sputtering not only can offer the possibility to prepare ITO films at low processing temperature on large areas[13], but also can obtain excellent optical and electrical properties. With the development of thin film technology, the photoelectrical properties of traditional binary ITO (In_2O_3:SnO_2) films can be improved by doping other elements. Besides tin, other elements such as Zr[14], Ti[15], Mo[16], W[17] and Ce[18] have also been employed as dopants. Among the researches, MoO_3 and WO_3 are easy to sublimate and difficult to be doped into In_2O_3

crystal structure. Titanium and zirconium have the same ionic valence with tin. Chung et al[19] have investigated the effect of titanium doping on the structural, optical and electrical properties of ITO:Ti films by direct current (DC) co-sputtering of metallic titanium and ceramic ITO target materials. Their results showed that the lowest resistivity is $2.3 \times 10^{-4}\,\Omega \cdot cm$, and the carrier concentration is 6.24×10^{20} cm⁻³. It is still a challenge to reduce the electrical resistivity and maintain the transmittance in visible range simultaneously.

In this paper, we demonstrate the control over the cationic composition in ITO-based oxide films by radio frequency (RF) magnetron sputtering using only one piece of niobium-doped ITO (ITO:Nb) ceramic target material in order to optimize the properties of the ITO:Nb films. The structural, electrical and optical properties of ITO:Nb films at different substrate temperatures are investigated.

The sputtering target material was made of ITO powder (99.99%) mixed with Nb_2O_5 powder (99.99%) through blending, moulding and sintering processes. The composition of In: Sn: Nb: O in ITO: Nb target materials is 66.31: 7.59: 0.77: 20.4 (wt%).

Corning Eagle 2000 (20 mm× 20 mm× 0.7 mm) glass, for

*   E-mail: maruixin@ustb.edu.cn

thin film transistor-liquid crystal display (TFT-LCD), was used as substrate to prepare ITO:Nb thin films by RF magnetron sputtering from as-prepared ITO:Nb ceramic target materials at RF power of 150 W. The target-substrate distance was 60 mm, and the base pressure in the sputtering chamber was 2×10^{-4} Pa. High pure argon gas (10 sccm, 99.999%) was introduced into sputtering chamber to maintain a working pressure of 0.80 Pa. All glass substrates were ultrasonically cleaned in acetone, ethanol and de-ionized water in turn, and then dried before sputtering. The sputtering was carried out for various substrate temperatures ranging from room temperature to 400 $^{\circ}$C.

The structural characteristics and morphology were performed by X-ray diffraction (XRD) and atomic force microscopy (AFM). The XRD spectra of all the films were recorded with Rigaku D/max-RB X-ray diffractometer (Rigaku, Tokyo, Japan, 40 kV, 150 mA) using Cu K$_{\alpha}$ radiation ($\lambda = 0.15406$ nm). The AFM imaging was performed under ambient conditions using a Digital Instrument (Veeco) Dimension-3100 unit with Nanoscope Ⓡ III controller, operating in tapping mode. The transmittances of the bare and the ITO:Nb-coated glass substrates were measured in the wavelength range from 300 nm to 800 nm by a spectrophotometer. Electrical resistivity, Hall mobility and carrier concentration of the ITO: Nb films were measured using a Van de Pauw method.

Typical XRD patterns of the as-prepared ITO:Nb thin films grown at different substrate temperatures are shown in Fig.1. Predominant characteristic peaks can be indexed to In$_2$O$_3$ crystalline phase (JCPDS 6-0416), which is in agreement with the previous work[20]. It illustrates that doping with niobium and tin does not result in the development of new crystal orientations or the changes of preferential orientations, which indicates that all samples are constituted of pure In$_2$O$_3$ phase, despite of the presence of niobium and tin dopant. This result implies that niobium and tin, which are added into the target materials, can not change the phase structure of In$_2$O$_3$ films and are doped into the crystal structure of In$_2$O$_3$. It is well known that the ITO films prepared with low oxygen proportion can achieve a crystalline cubic structure after annealing at 200 $^{\circ}$C, and different peaks can appear in XRD corresponding to (211), (222) and (400) crystal directions. Yang et al[20] reported similar crystalline properties with some amount of amorphous phase in the as-deposited ITO:Ti films. Chung et al[19] reported clear crystalline property with no amorphous phase in their as-deposited ITO:Ti films, which is in agreement with ITO:Nb films in this paper. In the case of ITO: Nb films, the intensity of XRD patterns shows more clear crystalline properties without amorphous phase even fabricated at room temperature without any processing after annealing. The strong crystalline growth in ITO:Nb films may be attrib-

uted to the Nb^{5+} and Ti^{4+} with small ionic radius, which is consistent with the experimental results of ITO:Ti films due to the similar ionic radius of Ti^{4+} (0.068 nm) and Nb^{5+} (0.069 nm). Therefore, it plays a key role in the strong crystalline growth of ITO: Nb film upon the doping of Nb^{5+} ions.
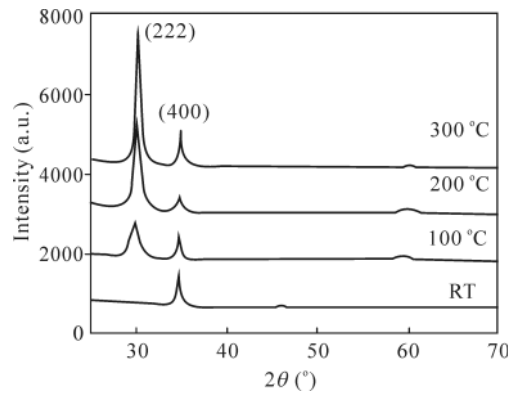

Fig.1 XRD patterns of ITO:Nb films at different substrate temperatures

The grain sizes of ITO:Nb films are calculated from the line broadening of (222) diffraction line according to the Scherrer equation[21] and shown in Fig.2. It can be observed that the lattice parameter of the films is reduced with the increasing of substrate temperature, while the crystallite size is increased with the increasing of substrate temperature.
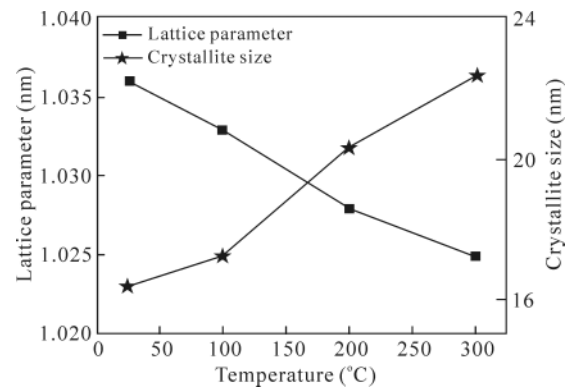

Fig.2 Lattice parameter and crystallite size of ITO: Nb films at different substrate temperatures

Besides the crystal structure, the surface morphology of ITO:Nb films was also measured using AFM. Fig.3 shows the AFM images of ITO:Nb films at different substrate temperatures. It is clear that the surface of the films is smoother at lower substrate temperature. With increasing of substrate temperature, the ITO:Nb grains begin to grow and cause the coarser surface, which is well consistent with the result of XRD measurements. Fig.4 shows the root mean square (RMS) roughness and average roughness of ITO:Nb thin films at different substrate temperatures. It is observed that the RMS

and average roughnesses of the film both increase with the increasing of substrate temperature. At room temperature, RMS and average roughnesses are 2.16 nm and 1.64 nm, respectively.
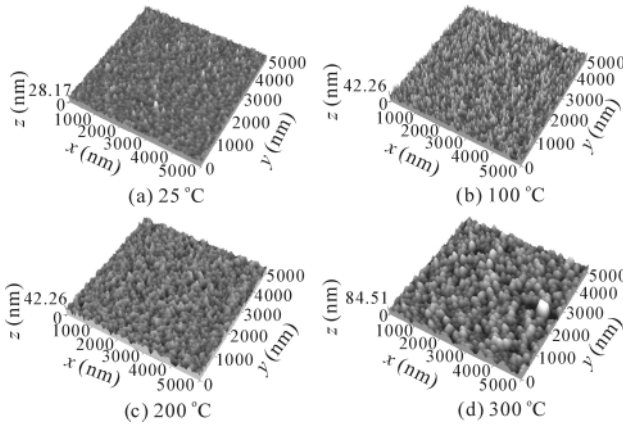

Fig.3 AFM images of ITO: Nb films at different substrate temperatures
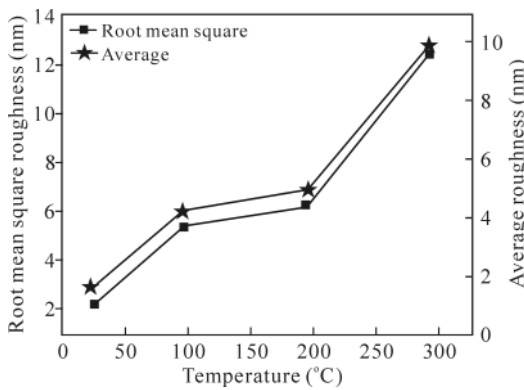

Fig.4 RMS and average roughnesses of ITO: Nb films at different substrate temperatures

The carrier concentration and Hall mobility of ITO:Nb at different substrate temperatures are shown in Fig.5. All the films have a similar thickness of 300−310 nm and the same composition confirmed by energy dispersive spectroscopy (EDS).
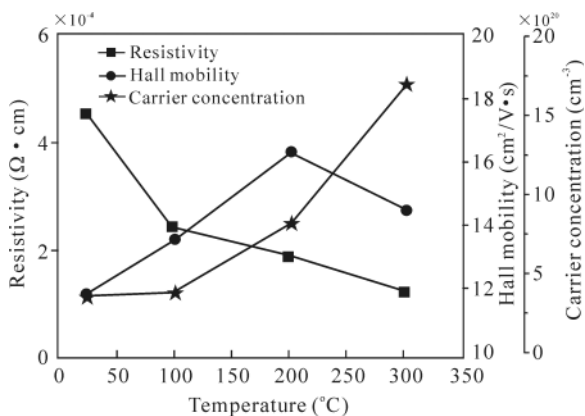

Fig.5 Electrical properties of ITO:Nb films at different substrate temperatures

Currently, the resistivity of ITO:Nb films is reduced while the substrate temperature rising. Especially, the lowest resistivity of ITO:Nb films is 1.2×10^{-4} Ù·cm when the substrate temperature is 300 °C. The decrease of resistivity of ITO:Nb films with increase of substrate temperature is ascribed to the crystallization and grain size, which leads to the reduction of grain boundary scattering, lattice defects, electron trap and the decrease in electrical resistivity[22]. In addition, there are a lot of adsorbed oxygen atoms accumulating on the grain boundaries at low substrate temperature. The adsorbed oxygen atoms are regarded as traps to capture free electrons and make the carrier concentration decrease. With the substrate temperature rising, the adsorbed atoms are desorbed from the grain boundaries and make the number of electronic capture traps decrease. Then, it improves the conductivity of the film.

It is found that the Hall mobility and carrier concentration are both increased with the increase of substrate temperature, and the maximum Hall mobility and carrier concentration are 16.5 cm²/V·s and 1.88×10^{21} cm⁻³, respectively.

Fig.6(a) shows the optical transmittance of ITO:Nb films at different substrate temperatures. The average transmittance is greater than 87% and the transmittance does not obviously change while substrate temperature changes. It is also observed from Fig.6 that the films exhibit the blue shift of the absorption edge in the ultraviolet region due to Burstein-Möss effect[23].

The band gap values of ITO:Nb films are calculated by the relation as

$$\alpha h \nu = A(h\nu - E_{g})^{n} , \qquad (1)$$

where $h\nu$ is the photon energy, α is the absorption coefficient, E_{g} is the band gap energy, A is the proportional coefficient, and n equals 1/2 for direct band-gap material. Fig.6(b) shows the relationship between $(\alpha h\nu)^2$ and $h\nu$ for ITO:Nb films at different substrate temperatures. It is found that the band gap is increased with the increase of substrate temperature. The calculated band gap energy values of ITO:Nb films at different substrate temperatures are listed in Tab.1.
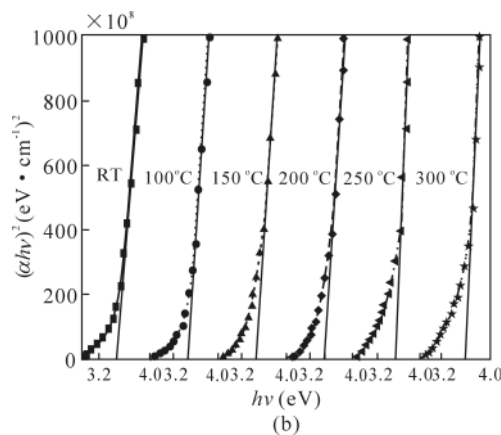

(a)
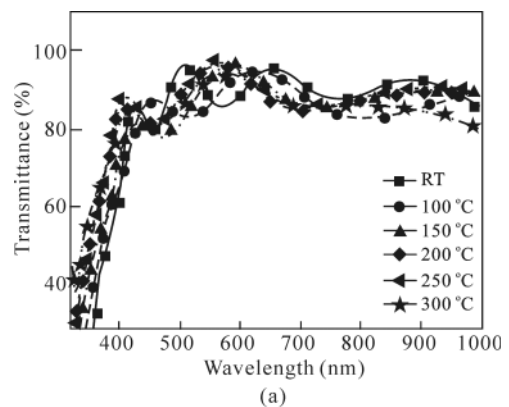
Fig.6 (a)Transmittance vs. wavelength and (b) ($\alpha h\nu$)^2 vs. ($h\nu$) at different substrate temperatures

Tab.1 Band gap of ITO:Nb film at different substrate temperatures

$T(^{\circ}C)$	RT	100	150	200	250	300
Band gap (eV)	3.49	3.58	3.58	3.59	3.61	3.63

ITO:Nb thin films are fabricated on glass substrates by RF magnetron sputtering at different temperatures from ceramic target materials. Structural, electrical and optical properties of the films are investigated using XRD, AFM, UV-VIS spectroscopy and electrical measurements. The XRD patterns show a polycrystalline structure in ITO:Nb films, which is similar to pure In_2O_3 phase, even deposited at room temperature. By increasing the substrate temperature, the intensity of (444) peak becomes weak gradually while it reverses for (222) peak. The AFM image shows a very smooth surface of ITO:Nb films. The optimized ITO:Nb film exhibits the lowest resistivity of 1.2×10^{-4} $\Omega \cdot cm$, the carrier concentration of 1.88×10^{21} cm^{-3} and the Hall mobility of 16.5 cm^2/V·s. All films have a transmittance of above 87%, indicating that such ITO:Nb films can be applied in various optical electronic devices.

References

[1]   A. E. Delahoy, L. Chen, M. Akhtar, B. Sang and S. Guo, Solar Energy **77**, 785 (2004).

[2]   C. P. Li, B. H. Yang, L. R. Qian, S. Xu, W. Dai, M. J. Li, X. W. Li and C. Y. Gao, Optoelectronics Letters **7**, 431 (2011).

[3]   R. X. Ma, Optoelectronics Letters **7**, 45 (2011).

[4]   R. B. H. Tahar, T. Ban, Y. Ohya and Y. Takahashi, J. Appl. Phys. **81**, 321 (1998).

[5]   E. Aperathitis, M. Bender, V. Cimalla, G. Ecke and M. Modreanu, J. Appl. Phys. **94**, 1258 (2003).

[6]   Y. F. Lan, W. C. Peng, Y. H. Lo and J. L. He, Materials Research Bulletin **44**, 1760 (2009).

[7]   L. J. Meng, J. Gao, M. P. dos Santosd, X. Wang and T. T. Wang, Thin Solid Films **516**, 1365 (2008).

[8]   J. P. Zheng and H. S. Kwok, Applied Physics Letters **63**, 1 (1993).

[9]   Y. Takahashi, S. Okada, R. B. H. Tahar, K. Nakano, T. Ban and Y. Ohya, Journal of Non-Crystalline Solids **218**, 129 (1997).

[10] T. Sasabayashia, N. Itoa, E. Nishimuraa, M. Kona, P. K. Songa, K. Utsumib, A. Kaijoc and Y. Shigesato, Thin Solid Films **445**, 219 (2003).

[11] A. Luis, C. Nunes de Carvalho, G. Lavareda, A. Amaral, P. Brogueira and M. H. Godinh, Vacuum **64**, 475 (2002).

[12] G. S. Belo, B. J. P. da Silva, E. A. de Vasconcelos, W. M. de Azevedo and E. F. da Silva Jr, Applied Surface Science **255**, 755 (2008).

[13] A. Amaral, P. Brogueira, C. Nunes de Carvalho and G. Lavareda, Journal of Nanoscience and Nanotechnology **10**, 2713 (2010).

[14] M. F. A. M. van Hest, M. S. Dabney, J. D. Perkins and D. S. Ginley, Applied Physics Letters **87**, 2111 (2005).

[15] S. H. Paeng, M. W. Park and Y. M. Sung, Surface and Coatings Technology **205**, 210 (2010).

[16] R. K. Gupta, K. Ghosh, R. Patel and P. K. Kahol, Applied Surface Science **255**, 6252 (2009).

[17] M. Yang, J. H. Feng, G. F. Li and Q. Zhang, Journal of Crystal Growth **310**, 3474 (2008).

[18] Y. M. Kang, S. H. Kwon, J. H. Choi, Y. J. Cho and P. K. Song, Thin Solid Films **518**, 3081 (2010).

[19] S. M. Chung, J. H. Shin, W. S. Cheong, C. S. Hwang, K. I. Choa and Y. J. Kim, Ceramics International **38**, s617 (2012).

[20] C. H. Yang, S. C. Lee, T. C. Lin and W. Y. Zhuang, Materials Science Engineering B **134**, 68 (2006).

[21] J. Yao, J. Shao, H. He and Z. X. Fan, Applied Surface Science **253**, 8911 (2007).

[22] H. Kim, J. S. Horwitz, G. P. Kushto, S. B. Qadri, Z. H. Kafafi and D. B. Chrisey, Appl. Phys. Lett. **78**, 1050 (2001).

[23] A. Sarkara, S. Ghosha, S. Chaudhuria and A. K. Pal, Thin Solid Films **204**, 255 (1991).